BPR MCS
Bulletin of Pioneering Researches of Medical and Clinical Science

Bulletin of Pioneering Researches of Medical and Clinical Science

Available online: https://bprmcs.com
2024 | Volume 4 | Issue 2 | Page: 138-145

Genetic and Immunohistochemical Evaluation of H3-3A Mutations for Diagnosing Giant Cell Bone Tumors

William J. Carter[1], Ahmed S. Farouk[2], Li Chen[1]*

[1]Department of Clinical Sciences, University of Sydney, Sydney, Australia.
[2]Department of Medical Sciences, Ain Shams University, Cairo, Egypt.

Abstract

This study aimed to assess the reliability of an objective diagnostic approach for giant cell tumour of bone (GCTB) by evaluating H3-3A gene mutations through Sanger sequencing and immunohistochemistry (IHC). The cohort comprised 214 patients: 120 diagnosed with GCTB and 94 with other giant cell-rich lesions of bone. Analyses were conducted on formalin-fixed, paraffin-embedded samples, with EDTA-based decalcification applied where required.
Sanger sequencing demonstrated 100% sensitivity (95 percent CI: 96.97–100 percent) and 100 percent specificity (95% CI: 96.15–100%). IHC using antibodies targeting histone H3.3 G34W and G34V variants showed 94.32% sensitivity (95 percent CI: 87.24–98.13 percent) and 100 percent specificity (95% CI: 93.94–100%). P.G35 mutations were identified in 2 of 9 (22.2 percent) secondary malignant GCTBs and 9 of 13 (69.2%) post-denosumab GCTB cases. In this extensive patient series, direct sequencing of H3-3A mutational status proved to be a highly dependable diagnostic tool for GCTB and warrants integration into standard diagnostic protocols. IHC serves effectively as a screening method, though accurate tissue handling and decalcification are essential. The detection of H3-3A mutations does not preclude malignancy in GCTB, and denosumab therapy does not eliminate the neoplastic cell population.

Keywords: Giant cell tumour of bone, H3-3A, H3F3A, Anti-histone H3.3 antibody, Denosumab

Corresponding author: Li Chen
E-mail: lichen@163.com

How to Cite This Article: Carter WJ, Farouk AS, Chen L. Genetic and Immunohistochemical Evaluation of H3-3A Mutations for Diagnosing Giant Cell Bone Tumors. Bull Pioneer Res Med Clin Sci. 2024;4(2):138-45. https://doi.org/10.51847/k52xuevexp

Introduction

Giant cell tumour of bone (GCTB) is a locally aggressive neoplasm, rarely metastatic, characterised by neoplastic mononuclear stromal cells admixed with macrophages and osteoclast-like giant cells. Its global incidence is estimated at 1.2–1.7 cases per million population annually, accounting for 5–8.6% of primary bone tumours [1–4]. It primarily occurs in skeletally mature individuals aged 20–45 years, most commonly in the epiphyseal regions of long bones (75–90%). Radiographically, GCTB appears as an eccentric, geographic osteolytic lesion with well-defined margins and no matrix mineralisation. The cortex may remain intact, show thinning/expansion, or be perforated, typically without periosteal reaction [5–9].

Pioneering work by Behjati *et al*. [10] and Presneau *et al*. [11] identified H3-3A gene mutations (formerly H3F3A) in 92 percent and 96 percent of GCTB cases, respectively, with Cleven *et al*. reporting 69% [12]. The H3-3A gene on chromosome 1 encodes the histone H3.3 variant, which constitutes 90 percent of histone H3 in post-mitotic mammalian cells and is expressed constitutively across the cell cycle [13, 14]. As a core nucleosome component, H3.3 influences gene expression via chromatin remodelling [15–18].

Per the NCBI/Consensus CDS reference (NM_002107.4; NP_002098.1), mutations in GCTB target codon 35 (p.Gly35), predominantly resulting in substitutions such as p.Gly35Trp, p.Gly35Leu, p.Gly35Arg, p.Gly35Met, p.Gly35Val, or p.Gly35Glu [10–12]. These mutations are generally sporadic and of unclear origin, though germline post-zygotic changes have been linked to rare syndromes involving pheochromocytoma, paraganglioma, and GCTB [19, 20].

Amary *et al*. established high specificity (90.6 percent) of commercial anti-histone H3.3 G34W monoclonal antibodies for IHC detection of p.Gly35 substitutions in GCTB [21]. Subsequent reports found no p.Gly35 mutations in most bone sarcomas (e.g., 0/28 cases [22]) or only rare occurrences in malignant bone tumours (e.g., 6/106 [23], 2/103 [10], 2/10 [11]). Clinical, radiological, and histological details for these mutated sarcomas remain limited, complicating exclusion of malignant GCTB.

Yamamoto *et al*. reported p.Gly35 mutations in all 51 conventional GCTB cases, both secondary malignant cases, and all eight denosumab-treated cases [24]. Yoshida *et al*. noted mutations in 28.5 percent (2/7) of malignant GCTB [25], while Girolami *et al*. confirmed them in 82% (9/11) of post-denosumab cases [26].

Gong *et al*. achieved 95% detection of H3-3A mutations in GCTB using combined IHC and molecular methods [27]. Kervarrec *et al*. identified mutations in 85 percent of cases [28]. Additional studies by Gong *et al*. [29] and Kato *et al*. [30] confirmed mutations in all nine post-denosumab cases examined via IHC or sequencing. Ogura *et al*. reported 96% mutation rate in typical GCTB, with two atypical cases lacking p.Gly35 but one harbouring an H3-3B p.G34V variant [31].

The present investigation evaluated the sensitivity and specificity of Sanger sequencing and IHC for H3-3A mutation detection in GCTB, drawing on thorough clinical, radiological, and histological characterisation. Conventional, malignant, and denosumab-treated GCTB cases were included, alongside mimics, to refine diagnostic criteria and assess the value of these molecular markers in differential diagnosis.

Results and Discussion

General characteristics of the GCTB cohort

Among the GCTB patients, the median age was 32 years (range: 10–81 years), with 3 percent younger than 19 years and 6% older than 60 years. Mean tumour size was 6.4 cm (range: 1.8–18 cm). Further details on the GCTB cohort are presented in **Table 1**.

Table 1. Characteristics of GCTB study group

Variable	Category	%	N
Sex	Male	48.7	58
	Female	51.3	61
Tumor site	Left	46.2	55
	Right	41.2	49
	Axial skeleton	12.6	15
Campanacci grade	Latent (I)	10.0	12
	Active (II)	58.0	69
	Aggressive (III)	32.0	38
Clinical course	No progression	78.2	93
	Progressive (recurrence or metastasis)	21.8	26

Molecular analysis

Analysis of the H3-3A gene by direct sequencing demonstrated that all tumours in the GCTB cohort carried a p.Gly35 mutation, while the control samples showed no mutations at codon 35 of the H3-3A gene **(Table 2)**.

Table 2. Results of direct Sanger sequencing.

		Study Cohorts		All	*p*-Value
		GCTB	Non-GCTB		
p.Gly35 mutation	yes	120 (100.0%)	0 (0.0%)	120 (56.1%)	<0.00001
	no	0 (0.0%)	94 (100.0%)	94 (43.9%)	

all	120 (100.0%)	94 (100.0%)	214 (100.0%)

The molecular assay demonstrated perfect sensitivity and specificity for identifying p.Gly35 mutations, with both measures at 100 percent (95 percent CI: 96.97–100 percent and 96.15–100 percent, respectively), and the findings were highly statistically significant ($p < 0.00001$). Among the tumours, 114 (95.0%) carried the p.Gly35Trp (G35W) alteration, which included all seven instances (100%) of GCTB affecting small tubular bones and one "atypical" GCTB case. A different p.Gly35Leu (G35L) mutation was detected in three tumours (2.5%), and the p.Gly35Val substitution was found in another three cases (2.5%). No additional p.Gly35 variants were observed in the H3-3A gene **(Figure 1)**.

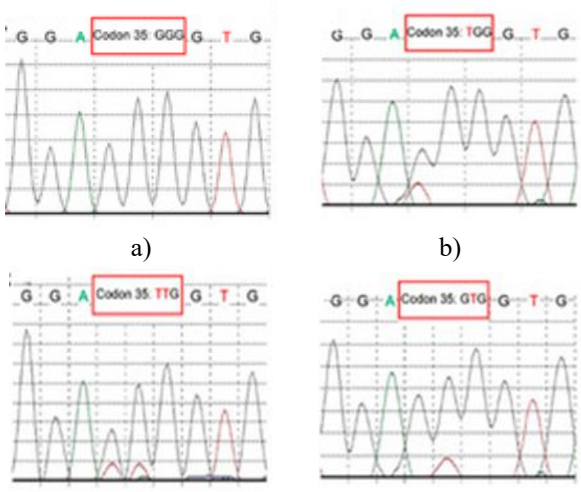

a) b) c) d)

Figure 1. Mutational spectrum of the H3-3A gene in giant cell tumour of bone (GCTB). (a) Wild-type H3-3A nucleotide sequence; (b) c.103G>T substitution at codon 35 leading to the p.Gly35Trp (G35W) mutation; (c) c.103_104delinsTT alteration at codon 35 resulting in the p.Gly35Leu (G35L) change; (d) c.104G>T variant at codon 35 corresponding to the p.Gly35Val (G35V) substitution.

IHC assays

Positive immunohistochemical results were defined exclusively by nuclear staining observed in the mononuclear tumour cells **(Figure 2)**.

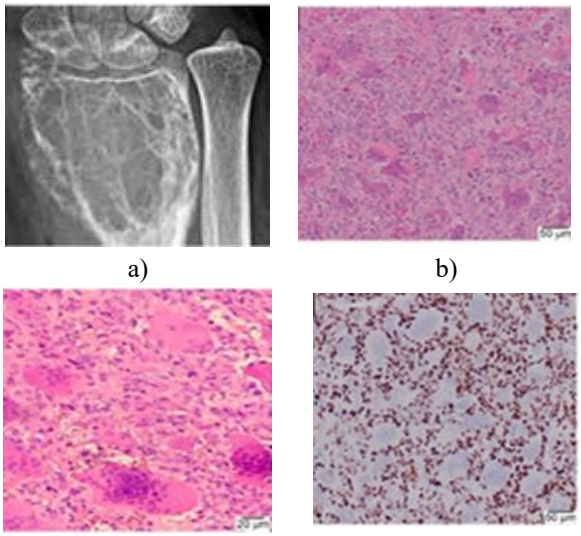

a) b) c) d)

Figure 2. Immunohistochemical evaluation using anti-histone H3.3 G34W antibody in GCTB cases with the p.Gly35Trp mutation. (a) Radiograph showing a typical osteolytic, epiphyseal, and locally aggressive GCTB lesion in the distal left radius; (b) conventional histology of GCTB revealing a relatively uniform distribution of osteoclast-like giant cells (H&E, 100×); (c) regions free of crush artifact displaying nuclear features of giant cells resembling those of mononuclear cells, with cells showing indistinct borders indicative of syncytial-like growth and no cytological atypia (H&E, 200×); (d) clear nuclear immunostaining in mononuclear tumour cells contrasted with the absence of nuclear staining in giant cells (IHC, 100×).

The IHC findings are summarized in **Table 3**.

Table 3. Immunohistochemical assay outcomes using anti-histone H3.3 G34W and G34V antibodies

Study Cohorts	Parameter	Non-GCTB	GCTB	Total	p-Value
Intensity	Positive (>0)	0 (0.0%)	83 (94.3%)	83 (56.5%)	<0.00001
	Negative (0)	59 (100.0%)	5 (5.7%)	64 (43.5%)	
	Total	59 (100.0%)	88 (100.0%)	147 (100.0%)	
Percentage	Positive (>0)	0 (0.0%)	83 (94.3%)	83 (56.5%)	<0.00001
	Negative (0)	59 (100.0%)	5 (5.7%)	64 (43.5%)	
	Total	59 (100.0%)	88 (100.0%)	147 (100.0%)	

The IHC assay demonstrated an estimated sensitivity of 94.32percent (95 percent CI: 87.24–98.13 percent) and specificity of 100% (95% CI: 93.6–100%), with the results reaching high statistical significance ($p < 0.00001$). All tumours carrying the p.Gly35Val (0/3) or p.Gly35Leu (0/3) mutations were negative when tested with the anti-

histone H3.3 G34W antibody, whereas GCTB cases with the p.Gly35Val substitution showed positive staining with the anti-histone H3.3 G34V antibody (3/3, 100 percent) **(Figure 3)**.

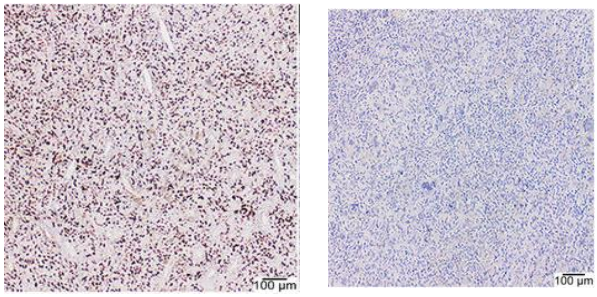

a) b)

Figure 3. GCTB cases harboring the p.Gly35Val mutation. (a) Positive immunostaining with the anti-histone H3.3 G34V antibody (IHC, 40×); (b) corresponding negative staining with the anti-histone H3.3 G34W antibody in the same tumour (IHC, 40×).

False-negative IHC results were noted in areas of degenerative change within the GCTB, such as secondary aneurysmal bone cysts, and following suboptimal decalcification of biopsy specimens (0/2) **(Figure 4)**.

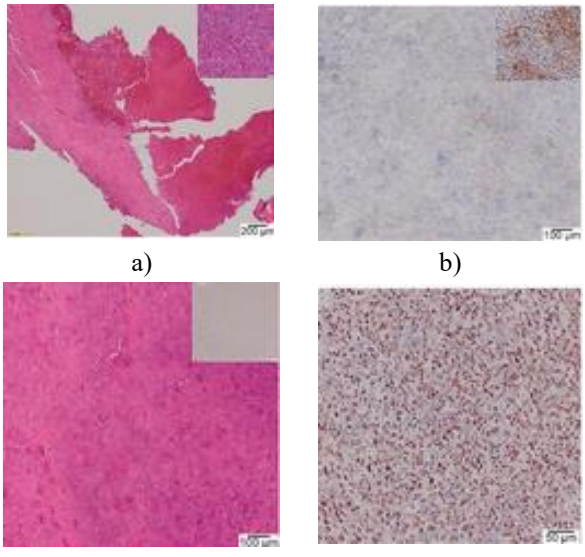

a) b)

c) d)

Figure 4. Areas of false-negative IHC staining in GCTB with p.Gly35Trp mutation using anti-histone H3.3 G34W antibody. (a) First case: secondary aneurysmal bone cyst formation, with an inset showing adjacent regions of typical GCTB histology (H&E, 20×); (b) lack of nuclear staining in the cystic region contrasted with positive staining in solid portions of the same tumour, captured from a different field (inset) (IHC, 40×); (c) Second case: recurrent GCTB exhibiting characteristic histology (H&E, 40×) with negative IHC following harsh acid decalcification, where molecular testing for p.Gly35 also failed—sample sent for expert review, and poor tissue preservation resulted in an empty counterstain appearance (inset); (d) subsequent rebiopsy with gentle EDTA decalcification restored positive nuclear staining, and sequencing confirmed the mutation (IHC, 100×).

Using both parameters of IHC evaluation—the staining intensity and proportion of positive tumour cells—the optimal threshold to differentiate GCTB from non-GCTB was established at 0. Assessments were highly reproducible between the two pathologists, with Cohen's kappa for intensity at 0.797 (95 percent CI: 0.713–0.881) and Spearman's correlation for percentage of positive cells at 0.914 ($p < 0.0001$). When using the cut-off of 0 for both parameters, pathologists achieved perfect concordance (Cohen's kappa = 1).

More than half of the GCTB cases demonstrated intermediate to strong IHC signals (2+ to 3+) by the Allred scoring system (pathologist I: 54.3 percent, pathologist II: 55.7 percent), with a median proportion of positive tumour cells of 60 percent (IQR, 40–70 percent).

H3-3A mutation analysis in GCTB after denosumab treatment

Out of 19 GCTB samples analyzed after denosumab therapy, 11 (57.9%) were positive for the p.Gly35 mutation, which was subsequently confirmed through immunohistochemistry **(Figure 5)**.

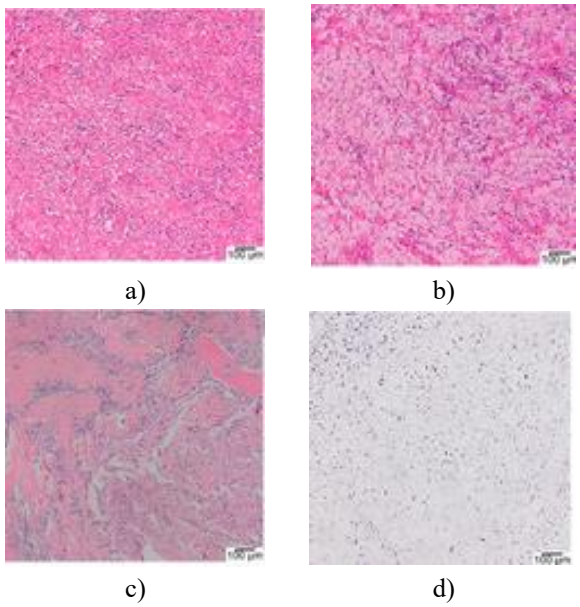

a) b)

c) d)

Figure 5. Morphological and IHC features of GCTB post-denosumab treatment. (a) Fibrotic changes within the stromal tissue (H&E, 40×); (b) presence of dispersed inflammatory cells, including foamy macrophages and lymphocytes (H&E, 40×); (c) spindle-shaped mononuclear cells with fibroblast-like appearance, absence of osteoclast-like giant cells, and localized ossification in the upper right corner (H&E,

40×); (d) immunohistochemical detection using anti-histone H3.3 G34W antibody on the same tissue section (40×).

H3-3A mutation analysis in malignant GCTB

Among the nine patients with secondary malignant GCTB, two cases (22.2%) exhibited the p.Gly35 variant in the H3-3A gene **(Figure 6)**.

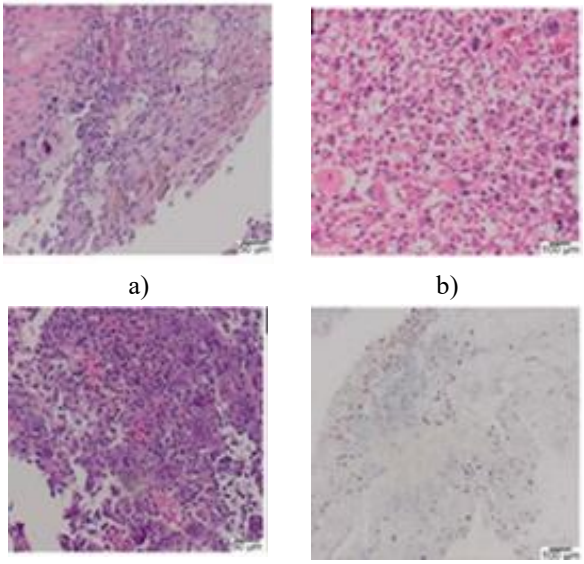

Figure 6. Secondary malignant GCTB in a 38-year-old male, occurring 14 years after radiotherapy for the primary lesion. (a, b) Marked sarcomatous atypia in tumour cells (H&E, 100× and 40×); (c) small areas retaining conventional GCTB histology (H&E, 40×); (d) nuclear positivity for anti-histone H3.3 G34W antibody (IHC, 100×), with molecular testing confirming the p.Gly35Trp mutation.

This study supports the use of molecular and immunohistochemical testing of H3-3A mutations for diagnosing GCTB, based on a substantial cohort including GCTB and other giant cell-rich bone lesions. Genetic analysis of H3-3A demonstrated nearly perfect sensitivity and specificity for GCTB detection, surpassing previously reported values. However, absence of a p.Gly35 mutation in tumour cells warrants cautious interpretation.

The investigation also highlighted that tissue processing can influence diagnostic accuracy. Proper EDTA-based decalcification is critical, as excessive decalcification can lead to false-negative molecular results.

Our findings indicate that only a subset of secondary malignant GCTB cases carry H3-3A mutations. Although the sample size for this group was limited, these data suggest that histopathological evaluation, together with radiological correlation, remains essential even when a p.Gly35 mutation is present.

Immunohistochemistry using commercially available anti-histone H3.3 antibodies showed slightly lower sensitivity than molecular analysis but offered high specificity, low cut-off thresholds, and strong interobserver concordance, making it a valuable screening tool. Each antibody specifically detected only one type of p.G35 substitution. False-negative IHC results were primarily associated with poorly processed specimens or areas of secondary aneurysmal bone cyst formation.

A limitation of the study was the lack of a commercially available antibody for detecting the p.Gly35Leu mutation, which was present in 2.5% of GCTB cases. Notably, none of these tumours occurred in the small tubular bones, contrasting with previous reports [11], highlighting the need for such antibody development. Primary malignant GCTB could not be analyzed, as none were identified during the study period, underscoring the need for further research.

Finally, the presence of p.Gly35-mutated tumour cells in over half of the GCTB cases after denosumab therapy confirms that anti-RANKL treatment does not eliminate the neoplastic population.

Materials and Methods

The study cohort included 214 patients: 120 with GCTB (including 19 evaluated after denosumab treatment), 9 with secondary malignant GCTB, and 94 with other giant cell-rich lesions (non-GCTB/control group).

The non-GCTB cohort comprised various pathologies: 29 osteosarcomas, 17 central giant cell granulomas, 15 primary aneurysmal bone cysts, 10 chondroblastomas, five brown tumours associated with hyperparathyroidism, four undifferentiated pleomorphic sarcomas, two tenosynovial giant cell tumours, one soft tissue giant cell tumour, two osteoblastomas, two non-ossifying fibromas, two fibrous dysplasias, two metastatic carcinomas, one benign fibrous histiocytoma, one low-grade fibrosarcoma with MDM2 amplification, and one non-specific granulation/bone fracture lesion. Samples collected from 2015–2018 underwent molecular analysis, while those from 2019–2020 were assessed by IHC; additional samples were included retrospectively and prospectively.

Radiological evaluation using X-ray, CT, and MRI was performed by board-certified musculoskeletal radiologists prior to histopathological examination. Select cases included measurement of serum calcium, phosphate, and parathyroid hormone levels.

Tissue specimens were obtained via core needle biopsy, open biopsy, or curettage, fixed in 10% neutral buffered formalin (pH 7.2–7.4) at room temperature for 12–24 hours, and processed using standard pathology protocols [32]. When decalcification was required, 10% buffered EDTA was applied at 36–37 °C using either a digital hotplate stirrer or incubator.

GCTB diagnosis required both radiologic and histologic criteria: (1) radiology showing eccentric, geographic

osteolytic lesions in long bone epiphyses, small tubular bones, vertebral bodies, sacrum, or skull base (excluding vertebral arcs and facial skeleton), and (2) histology revealing evenly distributed giant cells with nuclei resembling mononuclear cells, syncytial-like growth, absence of atypical mitoses, and minimal diffuse atypia.

Non-GCTB controls met at least one of the following: (1) did not satisfy GCTB criteria; (2) harboured alternative molecular alterations such as H3-3B or GNAS mutations, USP6 rearrangement, or MDM2 amplification; or (3) presented clinical signs of hyperparathyroidism.

All samples underwent Sanger sequencing of codon 35 in H3-3A. Selected cases were further analyzed for codon 201 in GNAS or codon 37 in H3-3B when fibrous dysplasia or chondroblastoma was suspected.

Paraffin-embedded tissue blocks were sectioned at 5–10 µm thickness using a microtome and subsequently deparaffinised. Only samples in which neoplastic tissue comprised at least 50% of the block were included, and macrodissection was performed when necessary. DNA extraction from non-decalcified or EDTA-decalcified specimens was carried out using the QiaAmp DNA Mini Kit (Qiagen, Hilden, Germany), whereas the Sherlock AX kit (A&A Biotechnology, Gdansk, Poland) was used for strongly acid-decalcified samples or tissues obtained after denosumab therapy. PCR amplification employed primers designed with Primer3 software (v4.1.0; https://primer3.ut.ee/; accessed 10 April 2016), avoiding regions with known variants and minor allele frequency ≥0.01% according to Ensembl (www.ensembl.org; accessed 10 March 2016). Sanger sequencing was conducted on an ABI Prism 3130 xl Genetic Analyzer (Applied Biosystems, Foster City, CA, USA) following standard protocols. Fluorograms were analyzed using Chromas (Technelysium Pty Ltd., South Brisbane, Australia) or FinchTV (Geospiza, Seattle, WA, USA), with mutation confirmation via Mutation Surveyor® Software (SoftGenetics, State College, PA, USA), using reference sequences NM_002107.4 (H3-3A), NM_005324.4 (H3-3B), and NM_000516.4 (GNAS). Codons exhibiting a double peak ≥10% of the normal allele were classified as positive for mutation.

Fluorescence in situ hybridisation (FISH) was performed on 19 denosumab-treated samples. Sections of 4 µm thickness were placed on two adhesive slides—one for FISH and one for H&E staining. Samples, either non-decalcified or EDTA-decalcified, with ≥100 neoplastic cells, were H&E-stained and evaluated by a pathologist. Commercial USP6 break-apart probes and MDM2/CEP12 probes (CytoTest, Rockville, MD, USA) were used, with visualization on an Olympus BX41 fluorescence microscope at 1000× with immersion. Filters included DAPI and spectrum-specific red/green channels to detect USP6 and MDM2 signals. Nuclei counts of 100 (USP6) and 60 (MDM2) were analyzed. Results were considered positive if ≥20% of cells exhibited USP6 rearrangement or if the MDM2/CEP12 ratio was ≥2.0.

IHC assays were subsequently conducted on 147 previously sequenced samples using rabbit monoclonal antibodies: anti-histone H3.3 G34W (clone RM263, 1:5000, pH 6.0) and anti-histone H3.3 G34V (clone RM307, 1:2000, pH 6.0) on an Autostainer Link 48 (Agilent) with EnVision FLEX/HRP detection. Two pathologists independently scored the percentage of positive mononuclear cells and staining intensity based on the Allred scoring system [33]. Images were captured with an Olympus BX43 microscope, SC50 digital camera, and cellSens software. Statistical analyses were performed using IBM SPSS Statistics 23.0.0.2 (SPSS Inc., Chicago, IL, USA).

Conclusion

The findings of this study support the use of direct Sanger sequencing as the definitive method for determining H3-3A mutational status in GCTB, while immunohistochemistry serves as an effective and reliable screening tool within the diagnostic workflow.

Acknowledgments: We would like to express our sincere gratitude to Monika Prochorec-Sobieszek for providing administrative and technical support.

Conflict of interest: None

Financial support: This research was funded by the Maria Sklodowska-Curie National Research Institute of Oncology, 5 Roentgen Str., 02-781 Warsaw, Poland (grant number SN/GW30/2017).

Ethics statement: The study was conducted in accordance with the Declaration of Helsinki guidelines. It was approved by the Institutional Ethics Committee of the Maria Sklodowska-Curie National Research Institute of Oncology, Warsaw, Poland (protocol code 7/2018, 8 February 2018).

Informed consent was obtained from all subjects involved in the study.

References

1. Flanagan AM, Larousserie F, O'Donnell PG, Yoshida A. Giant cell tumour of bone. In: WHO Classification of Tumours. Soft Tissue and Bone Tumours. 5th ed. Lyon: International Agency for Research on Cancer; 2020. p. 440–446.
2. Liede A, Bach BA, Stryker S, Hernandez RK, Sobocki P, Bennett B, et al. Regional variation and challenges in estimating the incidence of giant cell

tumor of bone. J Bone Joint Surg Am. 2014;96(23):1999–2007.
3. Unni KK. Tumors of the bones and joints. In: AFIP Atlas of Tumor Pathology. Washington (DC): Armed Forces Institute of Pathology; 2005.
4. Schajowicz F. Tumors and tumorlike lesions of bone: pathology, radiology, and treatment. Berlin: Springer; 1994.
5. Chakarun CJ, Forrester DM, Gottsegen C, Patel DB, White EA, Matcuk G. Giant cell tumor of bone: review, mimics, and new developments in treatment. Radiographics. 2013;33(1):197–211.
6. Balke M, Henrichs MP, Gosheger G, Ahrens H, Streitbuerger A, Koehler M, et al. Giant cell tumors of the axial skeleton. Sarcoma. 2012;2012(1):1–10.
7. Lee M, Sallomi D, Munk P, Janzen D, Connell D, O'Connell J, et al. Pictorial review: giant cell tumours of bone. Clin Radiol. 1998;53(7):481–9.
8. Lodwick GS, Wilson AJ, Farrell C, Virtama P, Dittrich F. Determining growth rates of focal lesions of bone from radiographs. Radiology. 1980;134(3):577–83.
9. Murphey MD, Nomikos GC, Flemming DJ, Gannon FH, Temple HT, Kransdorf MJ. Imaging of giant cell tumor and giant cell reparative granuloma of bone: radiologic-pathologic correlation. Radiographics. 2001;21(5):1283–309.
10. Behjati S, Tarpey PS, Presneau N, Scheipl S, Pillay N, Van Loo P, et al. Distinct H3F3A and H3F3B driver mutations define chondroblastoma and giant cell tumor of bone. Nat Genet. 2013;45(12):1479–82.
11. Presneau N, Baumhoer D, Behjati S, Pillay N, Tarpey P, Campbell PJ, et al. Diagnostic value of H3F3A mutations in giant cell tumour of bone compared to osteoclast-rich mimics. J Pathol Clin Res. 2015;1(2):113–23.
12. Cleven AH, Höcker S, Bruijn IB, Szuhai K, Cleton-Jansen AM, Bovée JV. Mutation analysis of H3F3A and H3F3B as a diagnostic tool for giant cell tumor of bone and chondroblastoma. Am J Surg Pathol. 2015;39(11):1576–83.
13. Wu RS, Tsai S, Bonner WM. Patterns of histone variant synthesis can distinguish G0 from G1 cells. Cell. 1982;31(2 Pt 1):367–74.
14. Hake SB, Garcia BA, Duncan EM, Kauer M, Dellaire G, Shabanowitz J, et al. Expression patterns and post-translational modifications associated with mammalian histone H3 variants. J Biol Chem. 2006;281(1):559–68.
15. Mariño-Ramírez L, Kann MG, Shoemaker BA, Landsman D. Histone structure and nucleosome stability. Expert Rev Proteomics. 2005;2(5):719–29.
16. Davey CA, Sargent DF, Luger K, Maeder AW, Richmond TJ. Solvent mediated interactions in the structure of the nucleosome core particle at 1.9 Å resolution. J Mol Biol. 2002;319(5):1097–113.
17. Griffiths AJF, Miller JH, Suzuki DT, Lewontin RC, Gelbart WM. Three-dimensional structure of chromosomes. In: An introduction to genetic analysis. 7th ed. New York: W.H. Freeman; 2000.
18. Felsenfeld G, Boyes J, Chung J, Clark D, Studitsky V. Chromatin structure and gene expression. Proc Natl Acad Sci U S A. 1996;93(18):9384–8.
19. Toledo R, Qin Y, Cheng ZM, Gao Q, Iwata S, Silva GM, et al. Recurrent mutations of chromatin-remodeling genes and kinase receptors in pheochromocytomas and paragangliomas. Clin Cancer Res. 2016;22(9):2301–10.
20. Toledo RA. Genetics of pheochromocytomas and paragangliomas: an overview on the recently implicated genes MERTK, MET, FGFR1, and H3F3A. Endocrinol Metab Clin North Am. 2017;46(2):459–89.
21. Amary F, Berisha F, Ye H, Gupta M, Gutteridge A, Baumhoer D, et al. H3F3A (histone 3.3) G34W immunohistochemistry: a reliable marker defining benign and malignant giant cell tumor of bone. Am J Surg Pathol. 2017;41(8):1059–68.
22. Righi A, Mancini I, Gambarotti M, Picci P, Gamberi G, Marraccini C, et al. Histone 3.3 mutations in giant cell tumor and giant cell–rich sarcomas of bone. Hum Pathol. 2017;68(1):128–35.
23. Koelsche C, Schrimpf D, Tharun L, Roth E, Sturm D, Jones DTW, et al. Histone 3.3 hotspot mutations in conventional osteosarcomas. Clin Sarcoma Res. 2017;7(1):9.
24. Yamamoto H, Iwasaki T, Yamada Y, Matsumoto Y, Otsuka H, Yoshimoto M, et al. Diagnostic utility of histone H3.3 G34W, G34R, and G34V mutant-specific antibodies for giant cell tumors of bone. Hum Pathol. 2018;73(1):41–50.
25. Yoshida KI, Nakano Y, Honda-Kitahara M, Wakai S, Motoi T, Ogura K, et al. Absence of H3F3A mutation in a subset of malignant giant cell tumor of bone. Mod Pathol. 2019;32(12):1751–61.
26. Girolami I, Mancini I, Simoni A, Baldi GG, Simi L, Campanacci D, et al. Denosumab-treated giant cell tumour of bone: a morphological, immunohistochemical and molecular analysis. J Clin Pathol. 2016;69(3):240–7.
27. Gong LH, Zhang W, Sun XQ, Zhang M, Ding Y. DNA sequencing of H3F3A mutations in H3.3 immunohistochemistry-negative giant cell tumors of bone. Zhonghua Bing Li Xue Za Zhi. 2021;50(3):190–3.

28. Kervarrec T, Collin C, Larousserie F, Bouvier C, Aubert S, Gomez-Brouchet A, et al. H3F3 mutation status of giant cell tumors of the bone, chondroblastomas and their mimics. Mod Pathol. 2017;30(3):393–406.
29. Gong L, Bui MM, Zhang W, Sun X, Zhang M, Yi D. H3F3A G34 mutation DNA sequencing and G34W immunohistochemistry analysis in 366 cases of giant cell tumors of bone and other bone tumors. Histol Histopathol. 2021;36(1):61–8.
30. Kato I, Furuya M, Matsuo K, Kawabata Y, Tanaka R, Ohashi K. Giant cell tumours of bone treated with denosumab: histological, immunohistochemical and H3F3A mutation analyses. Histopathology. 2018;72(6):914–22.
31. Ogura K, Hosoda F, Nakamura H, Hama N, Totoki Y, Yoshida A, et al. Highly recurrent H3F3A mutations with additional epigenetic regulator alterations in giant cell tumor of bone. Genes Chromosomes Cancer. 2017;56(10):711–8.
32. Grizzle WE. Special symposium: fixation and tissue processing models. Biotech Histochem. 2009;84(5):185–93.
33. Qureshi A, Pervez S. Allred scoring for ER reporting and its impact in clearly distinguishing ER-negative from ER-positive breast cancers. J Pak Med Assoc. 2010;60(5):350–3.